BIOMEDICAL SCIENCES

Type 2 diabetes mellitus alters cardiac mitochondrial content and function in a non-obese mice model

AINHOA R. DE YURRE, EDUARDA G.L. MARTINS, MICAELA LOPEZ-ALARCON, BRUNO CABRAL, NARENDRA VERA, JARLENE A. LOPES, ANTONIO GALINA, CHRISTINA M. TAKIYA, RAFAEL S. LINDOSO, ADALBERTO VIEYRA, OSCAR C. SÁENZ & EMILIANO MEDEI

Abstract: Type 2 diabetes mellitus (T2DM) is associated with an increase of premature appearance of several disorders such as cardiac complications. Thus, we test the hypothesis that a combination of a high fat diet (HFD) and low doses of streptozotocin (STZ) recapitulate a suitable mice model of T2DM to study the cardiac mitochondrial disturbances induced by this disease. Animals were divided in 2 groups: the T2DM group was given a HFD and injected with 2 low doses of STZ, while the CNTRL group was given a standard chow and a buffer solution. The combination of HFD and STZ recapitulate the T2DM metabolic profile showing higher blood glucose levels in T2DM mice when compared to CNTRL, and also, insulin resistance. The kidney structure/function was preserved. Regarding cardiac mitochondrial function, in all phosphorylative states, the cardiac mitochondria from T2DM mice presented reduced oxygen fluxes when compared to CNTRL mice. Also, mitochondria from T2DM mice showed decreased citrate synthase activity and lower protein content of mitochondrial complexes. Our results show that in this non-obese T2DM model, which recapitulates the classical metabolic alterations, mitochondrial function is impaired and provides a useful model to deepen study the mechanisms underlying these alterations.

Key words: Heart, high fat diet, mitochondria, streptozotocin, Type 2 diabetes.

INTRODUCTION

The prevalence and incidence of diabetes mellitus (DM) is increasing worldwide. Nowadays, the International Diabetes Federation calculates that there are more than 425 million people with diabetes and it is estimated that by the year 2045, approximately 629 million people will have diabetes (IDF 2017).

Type 2 diabetes mellitus (T2DM) is the most prevalent form of diabetes and about 90% of diabetic patients develop this syndrome, which is characterized by sustained high blood glucose levels and insulin resistance (Kaiser et al. 2018). This syndrome can lead to cardiovascular complications such as hypertension, coronary disease and stroke (Zimmet et al. 2001). Despite the advances in the treatment of this syndrome, there is still no effective treatment without secondary effects and this makes necessary to develop new strategies. For this, development of better animal T2DM models, which accurately reflect the pathogenesis of the human syndrome, are needed.

There exist several experimental T2DM models, of which rodents are the best choice

because of their short generation time. These models can be classified in spontaneous or genetic models and in induced models (Chatzigeorgiou et al. 2009, Srinivasan & Ramarao 2007). The spontaneous models are those bloodlines that remain relatively unaltered through inbred crosses that come either from an animal or from a series of selective crossings from an animal, where spontaneous diabetes has been detected or also, from a series of selective crossings promoting a certain phenotypic feature of human T2DM. Examples of these spontaneous T2DM mice models are the New Zeland Obese mouse (NZO), the db/db mouse or the ob/ob mouse among others. In contrast, the induced models are those in which T2DM is induced by chemicals (as alloxan or streptozotocin) or dietary manipulation, or by a combination of both (Srinivasan et al. 2005, Rees & Alcolado 2005). Even though this wide variety of animal models, most of them do not simulate accurately the human T2DM natural clinical history, besides being not easily achieved or affordable.

In the last decade, a model which combines a high fat diet (HFD) with low doses of a pancreatic β-cell toxin streptozotocin (STZ), has emerged as the best new alternative model that mimics the natural history of the progression of T2DM (Srinivasan & Ramarao 2007, Reed et al. 2000). The administration of HFD results in an insulin resistance situation, which is a key characteristic of T2DM. In addition, the low dose of STZ produces a partial β-cell dysfunction causing mild insulin secretion impairment. Thus, the combination of these two elements leads to a T2DM condition in experimental animals which is very close to the human one, even though in a shorter period of time. In addition, these models reflect the metabolic characteristics of human T2DM such as abnormalities in lipid

metabolism (Chatzigeorgiou et al. 2009, Reed et al. 2000, Li et al. 2015).

It is well known that approximately 65-70% of diabetic patients die due to cardiac alterations (Casis & Echevarria 2004, Laakso 2001, De Rosa et al. 2018). Mitochondrial dysfunction is the one of most related hypotheses of the cardiac dysfunction in diabetic individuals. Mitochondria represent around 30% of myocardial volume density (Schaper et al. 1985) and are responsible for generating about 60-90% of necessary energy for cardiomyocytes under form of high energy phosphoanhydride bonds in ATP and phosphagen by the fatty acid oxidation (Saddik et al. 1993). Thus, the metabolic imbalance induced by diabetes can cause mitochondrial dysfunction leading to early appearance of other cardiac alterations, and represent an important function to be evaluated in order to understand the molecular basis of the diabetic disease. In fact, previous observations in human hearts from T2DM patients presented decreased respiration rate in subsarcolemmal mitochondria (Croston et al. 2014). In a mouse model of T2DM a similar observation was detected (Koncsos et al. 2016). Nevertheless, in the present study we extended these evaluations including hydrogen peroxide (H_2O_2) release measurements and normalizing these data by specific mitochondrial content marker in our T2DM model.

Thus, the present work aims to test the hypothesis that a combination of HDF and two low doses of STZ recapitulate the natural history of the metabolic profile of T2DM, as well as the mitochondrial dysfunction. This model emerges as a new tool to study the early mechanisms underlying the cardiac alterations in non-obese T2DM as well as to test a new therapeutic approach.

MATERIALS AND METHODS

Animals and experimental protocol

All animal experiments were performed on adult C57BL/6 male mice in accordance with the Guide for the Care and Use of Laboratory Animals and approved by the Committee of the Federal University of Rio de Janeiro (protocol number 170/18). Animals were kept in controlled conditions of constant temperature (23 °C) and standard 12 h/12 h light/dark cycle with free access to water and chow.

Animals were divided in 2 groups: control non-diabetic mice (CNTRL) and type 2 diabetic mice (T2DM). CNTRL mice received a standard chow (Nuvilab, Brasil) consisting of 12% fat, 67% carbohydrate and 21% protein, with total calorific value of 3.33 Kcal/g. The T2DM mice group received a high fat diet (Pragsoluções Biociências, Jaú, SP, Brasil) consisting of 45% fat, 35% carbohydrates and 20% protein, with total calorific value of 4.73 Kcal/g. Two weeks after dietary establishment, T2DM mice received 2 consecutive injections of STZ (40 mg/kg/i.p.) (Sigma-Aldrich, St. Louis, MO, USA) diluted in 0.05 M citrate buffer (pH 4.5) separated 24 h, while CNTRL mice were given a vehicle (citrate buffer i.p.). Four weeks after injections biometric, functional, biochemical and molecular parameters were measured (Figure 1a). T2DM mice with the fasting blood glucose (FBG) higher than 140 mg/dl were considered diabetic. Both diets were maintained during the whole procedure for a total time of 6 weeks.

Fasting blood glucose, insulin, triglycerides and cholesterol concentration

FBG levels were measured using an automated glucometer (Contour™ TS Bayer HealthCare LLC, Mishawaka, IN, USA) with glucose reagent strips (Bayer HealthCare LLC). Animals were fasted for 6 h and blood was obtained from the tip of the tail of non-anesthetized mice. Insulin levels were measured using a commercial insulin RIA kit (ImmunoChem Coated Tube - Insulin – MP Biomedicals, Santa Ana, CA, USA) from blood serum samples.

Serum triglycerides (TG) and cholesterol levels were determined by enzymatic colorimetric method using commercial kits (Gold Analisa, Belo Horizonte, MG, Brasil).

Intraperitoneal glucose tolerance test, intraperitoneal insulin tolerance test and insulin resistance

For both, intraperitoneal glucose tolerance test (IPGTT) and intraperitoneal insulin tolerance test (IPITT), animals were fasted for 6 h and 4 h respectively. After that, animals were injected intraperitoneally 2 g/kg of glucose for IPGTT or 0.5 U/kg of insulin for IPITT and FBG was measured at different time points (0 (basal), 15, 30, 60 and 120 min) from a tail snip.

To assess insulin resistance, the HOMA-IR (homeostasis model assessment of insulin resistance) index was calculated as: fasting serum glucose x fasting serum insulin/22.5.

Histology and immunofluorescence

Kidney frozen sections were first fixed with 4% paraformaldehyde solution (20 min). After that, they were permeabilized with 0.5% triton X-100 in PBS, incubated with a blocking solution containing 1% glycine and 5% bovine serum albumin (BSA), and then with a neutrophil gelatinase-associated lipocalin (NGAL) rabbit polyclonal antibody (Abcam, Cambridge, MA, USA, cat # ab63929, 1:50) overnight. An anti-rabbit IgG F(ab')2 conjugated to Cy3 (Sigma-Aldrich, 1:200) was applied onto sections, washed with PBS, counterstained with DAPI (1:5000), and mounted with fluoromount.

RNA isolation and quantitative real-time polymerase chain reaction (qRT-PCR)

The RNA extraction from renal tissue was performed with mirVana RNA isolation kit (Thermo Scientific, Waltham, MA, USA) and RNA was measured spectrophotometrically (Nanodrop ND-1000, Thermo Scientific). mRNA expression was assessed using a High Capacity cDNA Reverse Transcription Kit (Applied Biosystems, Foster City, CA, USA), Power SYBR®Green PCR Master Mix (Applied Biosystems) and qRT-PCR was performed with a ViiA™ 7 Real-Time PCR System (Applied Biosystems). All the sequence-specific oligonucleotide primers (Supplementary Material - Table SI) were obtained from Thermo Scientific.

Biochemical analysis of the renal function

Blood urea nitrogen (BUN) and creatinine level were measured in plasma samples by the colorimetric method according to the manufacturer's protocol (K016, Bioclin, Belo Horizonte, Brazil).

Cytokines detection

IL-1β, IL-6 and TNF-α cytokines serum concentration was measured by a commercial ELISA kit (R&D systems Inc, Minneapolis, MN, USA) and results were obtained by a SpectraMax M3 equipment (Molecular Devices, San Jose, CA, USA).

Mitochondria isolation

Mitochondria isolation from the mice hearts was adapted from the protocol described by Affourtit et al. (2012) with minor modifications. The hearts were rapidly removed and rinsed in ice-cold Chappell-Perry (CP) buffer (100 mM KCl, 50 mM Tris-HCl, 2 mM EGTA, pH 7.2). Then, the hearts were blotted dry, weighed and finely minced with razor blades, and washed 4-5 times with CP buffer. The rinsed tissue was incubated for 5 min with CP buffer supplemented with 0.5% albumin, 5 mM $MgCl_2$, 1 mM ATP and 125 U/100 ml protease type VIII, at proportion 1 ml/100 mg of tissue. The minced tissue was homogenized (Ultra-turrax homogenizer (IKA®, Campinas, SP, Brasil), low setting, 3 s, 3 times) and the homogenate was centrifuged at 490 x g for 5 min. The resultant supernatant was centrifuged at 10368 x g for 10 min. The pellet was washed and resuspended into ice-cold CP buffer and centrifuged at 10368 x g for 10 min.

The final mitochondrial pellet was resuspended into 150-200 µl of CP buffer. The protein dosage of the isolated mitochondria as measured by the method described by Lowry et al. (1951). The isolated mitochondria were subjected to high resolution respirometry to measure the fluxes of oxygen consumption.

High resolution respirometry

The experiments were performed on the high-resolution O2k-respirometer (Oroboros Instruments, Innsbruck, Austria, EU) with mitochondrial respiration media (MIR05) containing 0.5 mM EGTA, 3 mM $MgCl_2$, 60 mM K-MES, 20 mM taurine, 10 mM KH_2PO_4, 20 mM HEPES, 110 mM sucrose, 1 g/l fat free BSA; pH 7.1 at 37 °C. The protocol used to evaluate mitochondrial function was adapted from Pesta & Gnaiger (2012) and consists on sequential addition of multiple substrates and inhibitors: 5 mM pyruvate, 2.5 mM malate, 10 mM glutamate, 100 µM adenosine 5'-diphosphate (ADP), 1 mM ADP, 10 mM succinate, 0.2 µg/ml oligomycin and 2 µM antimycin A (Ama).

The respiratory control ratio (RCR) was calculated by the oxygen flux after addition of succinate in presence of saturating concentrations of ADP, divided by the flux after oligomycin addition (satADP/Omy). The oxygen flux relative to complex I at phosphorylative state (CIp) was calculated by the flux in presence

of pyruvate, malate, glutamate and saturating ADP subtracting the residual oxygen flux (ROX, oxygen consumption not associated with the oxidative phosphorylation flux) which is the flux of oxygen obtained after the addition of Ama, a specific complex III inhibitor of mitochondria. The flux relative exclusively to complex II at phosphorylative state (CIIp) was determined by the respiration stimulated by succinate minus the flux in presence of saturating ADP and complex I substrates (CIp). The maximal oxidative phosphorylation capacity of the electron transport system (coupled to ATP synthesis -OXPHOS) was acquired subtracting the ROX from the flux with CI-linked substrates plus succinate and saturating ADP. The non-specific leak of protons (LEAK) was determined by oxygen flux after to oligomycin addition minus ROX.

The data were analysed in DatLab 5 software (Oroboros Instruments) and expressed in pmol. $mg^{-1}.sec^{-1}$.

Mitochondrial hydrogen peroxide release

The mitochondrial hydrogen peroxide (H_2O_2) production was measured by horseradish peroxidase/Amplex red coupled system. The appearance rate of resorufin at 563/587 nm (excitation/emission) was monitored in a fluorescence spectrophotometer (Varian Cary Eclipse, Agilent Technologies, Santa Clara, CA, USA). The assay was performed in 2 mL of MIR05 supplemented with 5.5 µM Amplex red, 2 U/ml peroxidase and 40 U/ml superoxide dismutase and 0.03 mg/ml of isolated mitochondrial at 37 °C. The H_2O_2 release at non-phosphorylative state was measured in presence of the same substrate concentrations of complex I and II, as mentioned above, for mitochondrial respiration. This condition induces a high electron potential to the ETS level, facilitating the monovalent reduction of oxygen and the production of

superoxide anion radical. These reactive oxygen species are rapidly converted in the H_2O_2, by non-limiting amounts of exogenous addition superoxide dismutase (SOD). The data generated in arbitrary units of fluorescence were analyzed in Origin Pro-8 software (Origin Lab Corporation, Northampton, MA, USA) and normalized to pmol of $H_2O_2.mg^{-1}.min^{-1}$ from standard calibration curves of H_2O_2 performed in the presence of the same amount of isolated mitochondria for each experiment.

Citrate synthase activity

The enzyme citrate synthase activity was measured, as described previously (Eigentler et al. 2015). The activity was determined by monitoring the reduction of 5,5-dithiobis 2-nitrobenzoic acid (DTNB) in a spectrophotometer at 420 nm (Victor plate reader, PerkinElmer, Waltham, MA, USA). The assay buffer was composed by 20 mM Tris-HCl, 0.3 mM DTNB, 2 mM EDTA and 0.3 mM acetyl-coenzyme A, pH 8.0. The reaction was initiated with 5 mM oxaloacetate. The generated data were analysed in Origin Pro-8 software (Origin Lab Corporation) and were expressed as $nmol.min^{-1}.mg^{-1}$.

Western blotting

Cardiac left ventricle were homogenized in lysis buffer (Tris-HCl 50 mM, pH 7.4 + NaCl 150 mM, EDTA 1 mM, Triton x-100 1%, Sodium deoxycholate 100 mM, SDS 1%, Sodium pyrophosphate 10 mM, NaF 100 mM, Sodium orthovanadate 10 mM and protease inhibitor cocktail) using the Ultra-Turrax T25 basic homogenizer (IKA®) at 9500 L/min. Samples were held on ice for 1 h and subsequently centrifuged at 12000 x g for 15 min at 4 °C. The supernatant was collected for protein dosage with Pierce™ BCA Protein Assay Kit (Thermo Fisher Scientific, Waltham, MA, USA) following manufacturer`s instructions. Samples (40 µg of total protein)

were resolved in SDS-PAGE 15% and transferred to a Polyvinylidene difluoride (PVDF) membrane (Bio-Rad, Hercules, CA, USA). After transfer, membrane was blocked with 5% nonfat dry milk for 2 h and incubated with anti-oxphos (Abcam) and anti-vinculin (Sigma-Aldrich), overnight at 4 °C. Then membrane was washed and incubated with HRP-conjugated specific secondary antibody (Invitrogen, Carlsbad, CA, USA) for 1 h at room temperature. Finally, membrane was developed using Amersham ECL Prime Western Blotting Detection Reagent (GE Healthcare Life Sciences, Pittsburgh, PA, USA). The capture of chemiluminescent signal was obtained using a Imagequant LAS4000 (GE Healthcare Life Sciences) equipment.

Statistical analysis

Data are presented as mean ± SEM. Comparison between 2 groups was analyzed by unpaired Student's t-test and multiple comparisons were performed using the analysis of two-way variance ANOVA and values of $p < 0.05$ were considered statistically significant. Samples sizes were estimated on the basis of sample availability and previous experimental studies of the cardiovascular system (Ferreiro et al. 2012, Monnerat et al. 2016). All analysis were performed using GraphPad Prism 7.0 (GraphPad Software, San Diego, CA, USA) and OriginPro8 (Origin Lab Corporation) softwares.

RESULTS

HFD and two low doses STZ recapitulate the T2DM metabolic profile

At the time, experimental T2DM models that try to reproduce the human diabetic cardiac alterations have several limitations that do not allow taking clear conclusions.

Six weeks after dietary establishment and STZ injection, animals with FBG higher than 140 mg/dl were considered diabetic and were used for the study (Figure 1b). Those T2DM animals showed similar serum insulin concentration to CNTRL group mice (Figure 1c). Even though T2DM mice were fed with a HFD, no exacerbated body weight gain was observed (Figure 1d). However, the slightly but significant higher body weight on T2DM mice when compared to CNTRL group was observed. This difference could be explained, at least in part, by the higher retroperitoneal and epididymal fat tissue measured on T2DM when compared to CNTRL group (Figure 1e, f). Also, serum TG and cholesterol concentration were higher in T2DM mice (Figure 1g, h).

In order to assess insulin resistance, HOMA-IR index, IPGTT and IPITT were performed. The data obtained here clearly demonstrate that T2DM mice were resistant to insulin, as showed by HOMA-IR index (Figure 1i) and by the AUC of both: IPGTT and IPITT (Figure 1j and k).

Collectively, these results showed that the combination of HFD with two low doses of STZ promoted a detriment of the metabolic state including a discrete increment of body weight, higher FBG and insulin resistance, characteristic conditions of a T2DM.

T2DM did not promote renal damage

Since T2DM is associated with renal diseases, we analyzed classical kidney damage and renal function markers (Figure 2). Both, right and left kidney showed similar weight in both groups (Figure 2a, b) and there was no renal atrophy (measured by relative kidney weight related to body weight index) (Figure 2c, d). The measurement of blood creatinine levels showed a mild increase in the T2DM condition with respect to the CNTRL; though, such difference was statistically significant (Figure 2e). The BUN level presented no difference between the
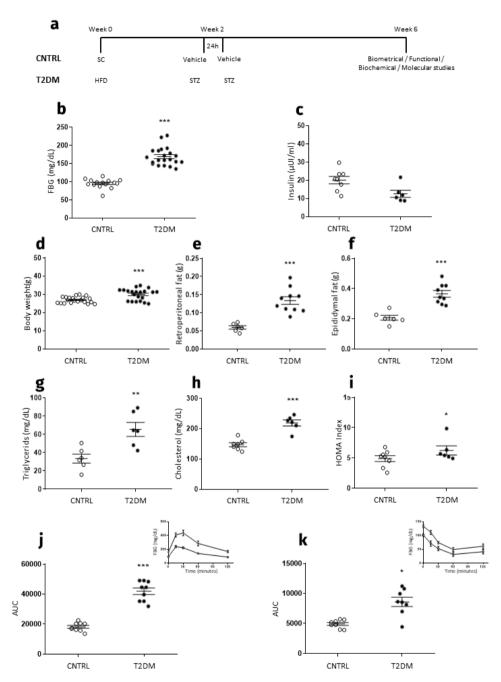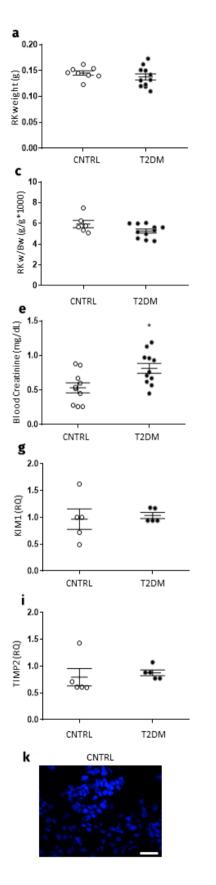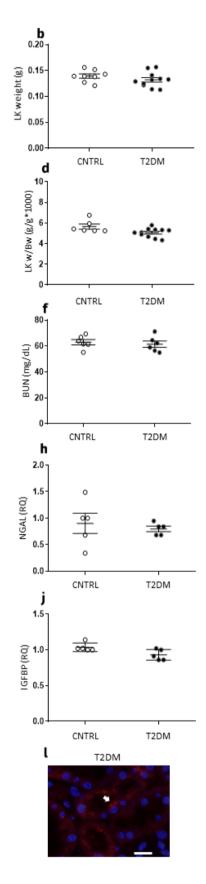
Figure 1. Combination of HFD and 2 low doses of STZ reproduce the metabolic alterations of T2DM. (a) T2DM experimental model establishment (CNTRL: Control; HFD: High Fat Diet (45% fat); SC: Standard Chow (4.15% fat); STZ: Streptozotocin (40 mg/kg); T2DM: Type 2 Diabetes Mellitus), (b) Fasting blood glucose (FBG) levels (CNTRL n = 15 mice and T2DM n = 21 mice), (c) Serum insulin concentration (CNTRL n = 8 mice and T2DM n = 6 mice), (d) Body weight (CNTRL n = 22 mice and T2DM n = 21 mice), (e) Retroperitoneal (CNTRL n = 6 mice and T2DM n = 10 mice) and (f) Epididymal fat (CNTRL n = 6 mice and T2DM n = 9 mice), Serum (g) Triglyceride (CNTRL n = 7 mice and T2DM n = 7 mice) and (h) Cholesterol (CNTRL n = 7 mice and T2DM n = 7 mice) concentrations, (i) HOMA index (FBG x FI / 22.5) (CNTRL n = 8 mice and T2DM n = 6 mice) and intraperitoneal (j) glucose (CNTRL n = 9 mice and T2DM n = 9 mice) and (k) insulin (CNTRL n = 9 mice and T2DM n = 9 mice) tolerance tests with the respective area under the curve (AUC) graphs 6 weeks after dietary establishment and STZ injection. Each dot represents individual values. ○: CNTRL mice; ●: T2DM mice. The results are shown as mean ± SEM. * $p < 0.05$; ** $p < 0.001$ and *** $p < 0.0001$ vs CNTRL.

Figure 2. T2DM present no renal functional or structural damage. Measurement of (a) right (RK - (CNTRL n = 8 and T2DM n = 11) and (b) left kidney (LK - (CNTRL n = 8 and T2DM n = 11)) weight. Relationship of (c) RK (CNTRL n = 6 and T2DM n = 11) and (d) LK (CNTRL n = 6 and T2DM n = 11) weight and body weight. (e) Blood creatinine (CNTRL n = 11 and T2DM n = 11) and (f) BUN (CNTRL n = 6 and T2DM n = 6) levels in T2DM and CNTRL animals. mRNA levels (n = 5 per group) of (g) KIM-1, (h) NGAL, (i) TIMP-2 and (j) IGFBP7 in renal tissue expressed as RQ in respect to CNTRL group. Representative photomicrographies of kidney sections (Cortex): (k) Cortex from control mice – lack of NGAL immunostaining, (l) Cortical tubular epitelial cell from T2DM mice showing rare punctate NGAL staining (arrow). Bar: 50 μm. Each dot represents individual values. ○: CNTRL mice; ●: T2DM mice. The results are shown as mean ± SEM.

groups (Figure 2f), indicating no alteration in the renal function in T2DM animals.

The mRNA levels of key markers associated with tissue damage were also assessed (Figure 2g-j). KIM-1 and NGAL, markers of acute kidney damage, were not regulated by T2DM (Figure 2g, h). The NGAL gene expression results also were confirmed by immunofluorescence. Conversely to gene expression, the immunofluorescence depicted, even though that slightly, some NGAL expression, as showed in Figure 2k and l. As markers for kidney chronic diseases, TIMP-2 and IGFBP7 that are associated with fibrosis and epithelial-to-mesenchymal transition process, were evaluated. T2DM animals did not present any difference in the mRNA levels when compared to the CNTRL group in both cases (Figure 2i, j). Together, these results indicate that during this period of analysis (6 weeks), the T2DM model developed here did not lead to kidney damage.

T2DM model induces changes in the immune response

It is widely accepted that T2DM induces a pro-inflammatory response, classically a non-infectious disease (Spranger et al. 2003). Here we measure the circulating levels of three pivotal cytokines. Thus, the present T2DM mice model showed an increment of IL-1β and IL-6, without differences on the TNF-α levels (Figure 3a-c).

Collectively this data suggest that the T2DM mice model recapitulate the typical immune disorder induced in this disease.

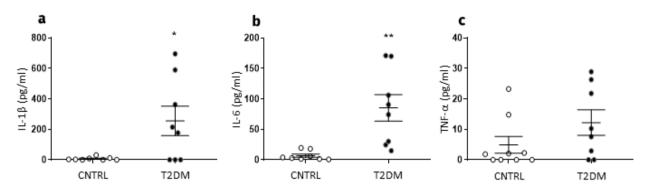### T2DM decreases electron transport system oxygen consumption by mitochondrial content reduction

In several metabolic diseases where the cardiac function is impaired, the mitochondrial structure/function plays a vital role (Luptak et al. 2019). To analyse the mitochondrial function,
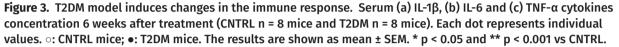
we first performed a protocol with multiple substrates and inhibitors to measure oxygen flux consumed by mitochondria at different respiratory states. We also performed the measurement of H_2O_2 production to assess the electron leakage by the electron transport system (ETS) during non-phosphorylative respiratory state. The differences between the mitochondrial oxygen consumption from CNTRL and T2DM mice are shown in Figure 4. No significant difference in RCR, factor related to the oxidative phosphorylation coupling efficiency of ETS, was detected (Figure 4a). However, in all phosphorylative states (CI_p, CII_p and OXPHOS), the cardiac mitochondria from T2DM mice presented reduced oxygen fluxes (22%, 13% and 18%, respectively) when compared to CNTRL mice (Figure 4b-d). No significant changes were detected on LEAK, state related to non-specific protons leak (Figure 4e).

The electron transport through the ETS favours electron leak in various sites of mitochondria generating superoxide, which is rapidly converted to H_2O_2. Thus, as showed in Figure 4f, significant decreased H_2O_2 production rates were observed in T2DM animals (27%) compared to CNTRL ones.

Citrate synthase (CS) is commonly used as quantitative marker of mitochondrial content (Mogensen et al. 2006). As observed in Figure 4g, mitochondria from T2DM mice showed decreased CS activity (19%).

Since the mitochondrial activity is highly associated to the mitochondrial content, we performed the normalization of respiratory fluxes of oxygen and H_2O_2 production by the CS activity. The normalized data showed in Figure 4h-l, strongly suggest that the changes observed were due to lower mitochondria content. In addition, in line with the CS activity, the protein content of mitochondrial complexes
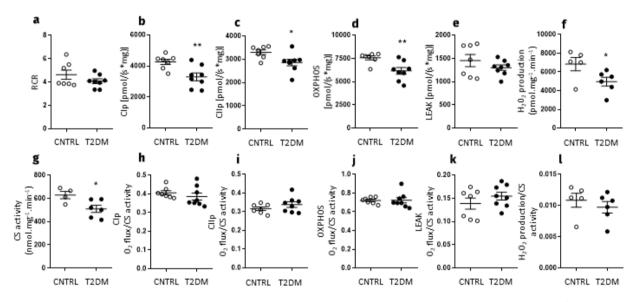
Figure 3. T2DM model induces changes in the immune response. Serum (a) IL-1β, (b) IL-6 and (c) TNF-α cytokines concentration 6 weeks after treatment (CNTRL n = 8 mice and T2DM n = 8 mice). Each dot represents individual values. ○: CNTRL mice; ●: T2DM mice. The results are shown as mean ± SEM. * p < 0.05 and ** p < 0.001 vs CNTRL.

Figure 4. T2DM decreases oxygen flux and H_2O_2 production rate by reduction of mitochondrial content. (a) Respiratory control ratio (RCR), (b) oxygen flux in phosphorylative state with complex I linked substrates, (c) oxygen flux in phosphorylative state with complex II linked substrate, (d) maximal phosphorylative capacity of ETS, (e) non-specific leak of protons, (f) H_2O_2 production in non-phosphorylative state, (g) quantification of citrate synthase activity. (h, i, j, k and l) normalized data by the citrate synthase activity of graphs b, c, d, e and f, respectively (CNTRL n = 4 - 7 hearts and T2DM n = 6 - 8 hearts). Each dot represents independent mitochondrial isolation from one heart. ○: CNTRL mice; ●: T2DM mice. The results are shown as mean ± SEM. * p < 0.05 and ** p < 0.001 vs CNTRL.

was drastically reduced between 12 to 37%, as demonstrated in Figure 5b-f.

The set of experiments performed depicts that T2DM mice model was able to decrease the mitochondrial content and consequently, decrease the cardiac mitochondrial performance.

DISCUSSION

Although approximately 90% of the diabetic patients develop T2DM (Zheng et al. 2018), most of the experimental works to study the mechanism of the cardiac damage induced by this disease have been performed in T1DM
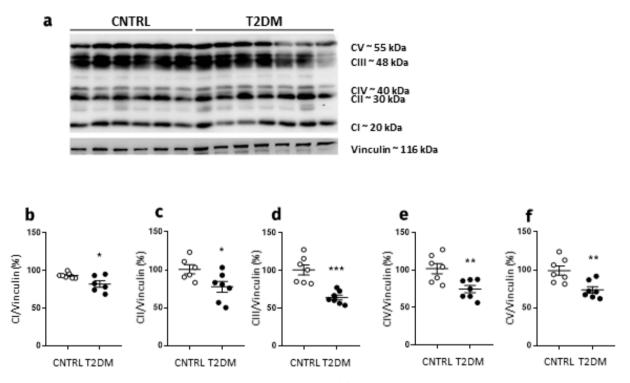
Figure 5. T2DM depicts lower cardiac mitochondria complexes. (a) Western-blott assay and the representative graphs of protein content of mitochondrial (b) Complex I, (c) Complex II, (d) Complex III, (e) Complex IV and (f) Complex V. Each dot represents independent mitochondrial isolation. ○: CNTRL mice; ●: T2DM mice. CNTRL n = 7 hearts and T2DM n = 6 - 7 hearts. The results are shown as mean ± SEM. * p < 0.05 and ** p < 0.001 vs CNTRL. Each symbol represents an independent mitochondria preparation from one heart.

animal models (Casis et al. 2000, Torres-Jacome et al. 2013), demonstrating the lack of a suitable T2DM animal model. Therefore, the data obtained here allow us to propose a new T2DM mice model that mimics the natural history of this syndrome in humans to deepen study the metabolic and cardiac characteristics.

Previous studies have reported the use of the combination of a high fat diet (HFD) and low dose of streptozotocin (STZ) to induce T2DM in experimental animal models (Srinivasan & Ramarao 2007, Reed et al. 2000, Li et al. 2015). Nevertheless, there are still methodology variations concerning to dietary administration period prior to STZ injection and, overall, to the administered STZ dose (Srinivasan & Ramarao 2007, Reed et al. 2000). In the present study, we successfully obtained a T2DM mice model

which mimics an end stage of the human T2DM, obtained in a short period of time.

Usually, T2DM mice models are associated to obesity derived from metabolic syndrome (Srinivsan et al. 2005). Here, despite HFD feeding, T2DM mice have not shown an exacerbated body weight gain, but present higher visceral fat mass percentage when compared to CNTRL group, as it is described to non-obese T2DM patients (Vaag & Lund 2007).

It is well described that T2DM patients, in advanced stages of the disease develop several problems such as cardiovascular complications, microangiopathy, retinopathy, neuropathy or nephropathy. Indeed, T2DM is the leading cause of end stage renal disease, which increases the risk of death among patients with diabetes (Brancati et al. 1997, Finne et al. 2019). Wu et al. (2010) in a

T2DM aging mice showed that renal impairment was due in part to the excessive stress and inflammation derived from the aging process and that diabetes may accelerate the underlying kidney aging process present in old mice (Wu et al. 2010). When we evaluate renal morphology and function through kidney damage markers and biochemical measurements, no renal functional or tissue damage was observed, even though slightly NGAL expression was observed, which lead us to propose that our T2DM model, at least in 6 weeks, would not present a typical chronic stage of the T2DM disease.

In the last decade the study of the role of inflammatory responses in the physiopathology of T2DM has increased (Herder et al. 2015). Several works described that IL-1β contribute not only to impair the β-cell function (Maedler et al. 2002) but also cardiac function (Monnerat et al. 2016, Fernández-Sada et al. 2017). In this regards, different clinical trials are actually ongoing in order to understand the potential therapeutic role of this cytokine (Zhao et al. 2014). In this sense, we observed an increase of IL-1β and IL-6 in T2DM mice. This could lead us to think that these cytokines may play an essential role in the pathophysiology of this disease that needs to be studied in depth.

Furthermore, it is well described that metabolic disturbance is a typical finding in T2DM (Wang et al. 2010). In this regards, mitochondrial dysfunction can play a critical role in the development of T2DM related disturbances. However, if the energetic deficit of cardiac tissue is due to insufficient or to defective mitochondrial function, which can play a pathogenic role on T2DM (Szendroedi et al. 2011) is yet a debate. Koncsos et al. (2016) described, in a prediabetes state, that early changes in several phenomena such as changes in cardiac mitophagy and elevated subsarcolemmal mitochondria reactive oxygen species production may be responsible

for prediabetic cardiac complications. This leads us to propose that in a diabetic state, these phenomena still persist (Koncsos et al. 2016). Our measurements showed that T2DM mitochondrial H_2O_2 released is lower when compared to CTRL, but correlates with the decreased levels (less 20-30%) in mitochondrial content (Figure 4). This apparent contradiction is explained by the fact that: 1- The work performed by Koncsos et al. (2016) evaluated mitochondrial H_2O_2 in a pre-diabetic state; 2- in that study it was used the subsarcolemmal preparations of mitochondria; and finally 3- in this previous study the high H_2O_2 released from mitochondria was only observed in the presence of CI-linked substrates.

Concurrent with this, here we observed that the lower mitochondria response was due to lower mitochondrial content and complex of ETS abundance, as showed by citrate synthase activity and the Western-blotting assay (Figures 4-5). These results allow us to suggest that the impairment on cardiac mitochondrial function observed in the T2DM model, was due to lower mitochondrial content and not to a specific mitochondrial dysfunction attributable to altered mitochondria function. A similar observation was seen in skeletal human permeabilized muscle fibers from biopsies of the quadriceps of T2DM patients, in which no mitochondrial dysfunction, but lower content was detected (Boushel et al. 2007). In line with our results, Marciniak et al. (2014) found that mice fed with HFD that received or not STZ was associated with a dramatic reduction in mitochondrial respiration (Marciniak et al. 2014). Other recent study (Croston et al. 2014) with T2DM in human cardiac biopsies showed decreased oxidative phosphorylation function and CI and CIV complex levels specifically subsarcolemmal mitochondria.

In summary, the results showed here demonstrate that in this non-obese T2DM model

cardiac mitochondrial function is impaired as a consequence of lower mitochondrial content, recapitulating the mitochondrial impairment previously described in human skeletal muscle obtained from T2DM patients. Therefore, this T2DM mice model emerge as a great tool for deepen study the mechanisms underlying these alterations and allows future investigations of the molecular energetic basis of diabetes disease.

Acknowledgments

REFERENCES

AFFOURTIT C, QUINLAN CL & BRAND MD. 2012. Measurement of proton leak and electron leak in isolated mitochondria. Methods Mol Biol 810: 165-182.

BOUSHEL R, GNAIGER E, SCHJERLING P, SKOVBRO M, KRAUNSØE R & DELA F. 2007. Patients with type 2 diabetes have normal mitochondrial function in skeletal muscle. Diabetologia 50(4): 790-796.

BRANCATI FL, WHELTON PK, RANDALL BL, NEATON JD, STAMLER J & KLAG MJ. 1997. Risk of end-stage renal disease in diabetes mellitus: a prospective cohort study of men screened for MRFIT. Multiple Risk Factor Intervention Trial. JAMA 278(23): 2069-2074.

CASIS O & ECHEVARRIA E. 2004. Diabetic cardiomyopathy: electromechanical cellular alterations. Curr Vasc Pharmacol 2(3): 237-248.

CASIS O, GALLEGO M, IRIARTE M & SÁNCHEZ-CHAPULA JA. 2000. Effects of diabetic cardiomyopathy on regional electrophysiologic characteristics of rat ventricle. Diabetologia 43(1): 101-109.

CHATZIGEORGIOU A, HALAPAS A, KALAFATAKIS K & KAMPER E. 2009. The use of animal models in the study of diabetes mellitus. *In vivo* 23(2): 245-258.

CROSTON TL ET AL. 2014. Functional deficiencies of subsarcolemmal mitochondria in the type 2 diabetic human heart. Am J Physiol Heart Circ Physiol 307(1): H54-H65.

DE ROSA S, ARCIDIACONO B, CHIEFARI E, BRUNETTI A, INDOLFI C & FOTI DP. 2018. Type 2 Diabetes Mellitus and Cardiovascular Disease: Genetic and Epigenetic Links. Front Endocrinol 9: 2-15.

EIGENTLER A, DRAXL A, WIETHÜCHTER A, KUZNETSOV AV, LASSNIG B & GNAIGER E. 2015. Laboratory protocol: citrate synthase, a mitochondrial marker enzyme. Mitochondrial Physiology Network 17(04): 1-11.

FERNÁNDEZ-SADA E ET AL. 2017. Proinflammatory cytokines are soluble mediators linked with ventricular arrhythmias and contractile dysfunction in a rat model of metabolic syndrome. Oxid Med Cell Longev 2017: 12.

FERREIRO M, PETROSKY AD & ESCOBAR AL. 2012. Intracellular Ca^{2+} release underlies the development of phase 2 in mouse ventricular action potentials. Am J Physiol Heart Circ Physiol 302(5): H1160-H1172.

FINNE P, GROOP PH, ARFFMAN M, KERVINEN M, HELVE J, GRÖNHAGEN-RISKA C & SUND R. 2019. Cumulative Risk of End-Stage Renal Disease Among Patients With Type 2 Diabetes: A Nationwide Inception Cohort Study. Diabetes Care 42(4): 539-544.

HERDER C, DALMAS E, BÖNI-SCHNETZLER M & DONATH MY. 2015. The IL-1 Pathway in Type 2 Diabetes and Cardiovascular Complications. Trends Endocrinol Metab 26(10): 551-563.

IDF. 2017. International Diabetes Federation, IDF Diabetes Atlas, 8th ed., International Diabetes Federation.

KAISER AB, ZHANG N & VAN DER PLUIJM W. 2018. Global Prevalence of Type 2 Diabetes over the Next Ten Years (2018-2028). Diabetes 67(Suppl 1): 202-LB.

KONCSOS G ET AL. 2016. Diastolic dysfunction in prediabetic male rats: Role of mitochondrial oxidative stress. Am J Physiol Heart Circ Physiol 311(4): H927-H943.

LAAKSO M. 2001. Cardiovascular disease in type 2 diabetes: challenge for treatment and prevention. J Intern Med 249(3): 225-235.

LI Y, JI DF, ZHONG S, LIN TB & LV ZQ. 2015. Hypoglycemic effect of deoxynojirimycin-polysaccharide on high fat diet and streptozotocin-induced diabetic mice via regulation of hepatic glucose metabolism. Chem Biol Interact 225: 70-79.

LOWRY OH, ROSEBROUGH NJ, FARR AL & RANDALL RJ. 1951. Protein measurement with the Folin phenol reagent. J Biol Chem 193(1): 265-275.

LUPTAK I ET AL. 2019. Energetic dysfunction is mediated by mitochondrial Reactive Oxygen Species and precedes structural remodeling in metabolic heart disease. Antioxid Redox Signal 31(7): 539-549.

MAEDLER K, SERGEEV P, RIS F, OBERHOLZER J, JOLLER-JEMELKA HI, SPINAS GA, KAISER N, HALBAN PA & DONATH MY. 2002. Glucose-induced beta cell production of IL-1beta contributes to glucotoxicity in human pancreatic islets. J Clin Invest 110(6): 851-860.

MARCINIAK C, MARECHAL X, MONTAIGNE D, NEVIERE R & LANCEL S. 2014. Cardiac contractile function and mitochondrial respiration in diabetes-related mouse models. Cardiovasc Diabetol 13: 118-129.

MOGENSEN M, BAGGER M, PEDERSEN PK, FERNSTRÖM M & SAHLIN K. 2006. Cycling efficiency in humans is related to low UCP3 content and to type I fibres but not to mitochondrial efficiency. J Physiol 571(Pt 3): 669-681.

MONNERAT G ET AL. 2016. Macrophage-dependent IL-1β production induces cardiac arrhythmias in diabetic mice. Nat Commun 7: 13344-13359.

PESTA D & GNAIGER E. 2012. High-resolution respirometry: OXPHOS protocols for human cells and permeabilized fibers from small biopsies of human muscle. Methods Mol Biol 810: 25-58.

REED MJ, MESZAROS K, ENTES LJ, CLAYPOOL MD, PINKETT JG, GADBOIS TM & REAVEN GM. 2000. A new rat model of type 2 diabetes: the fat-fed, streptozotocin-treated rat. Metabolism 49(11): 1390-1394.

REES DA & ALCOLADO JC. 2005. Animal models of diabetes mellitus. Diabet Med 22(4): 359-370.

SADDIK M, GAMBLE J, WITTERS LA & LOPASCHUK GD. 1993. Acetyl-CoA carboxylase regulation of fatty acid oxidation in the heart. J Biol Chem 268(34): 25836-25845.

SCHAPER J, MEISER E & STÄMMLER G. 1985. Ultrastructural morphometric analysis of myocardium from dogs, rats, hamsters, mice and from human hearts. Circ Res 56(3): 377-391.

SPRANGER J, KROKE A, MÖHLIG M, HOFFMANN K, BERGMANN MM, RISTOW M, BOEING H & PFEIFFER AF. 2003. Inflammatory cytokines and the risk to develop type 2 diabetes: results of the prospective population-based European Prospective Investigation into Cancer and Nutrition (EPIC)-Potsdam Study. Diabetes 52(3): 812-817.

SRINIVASAN K & RAMARAO P. 2007. Animal models in type 2 diabetes research: an overview. Indian J Med Res 125(3): 451-472.

SRINIVASAN K, VISWANAD B, ASRAT L, KAUL CL & RAMARAO P. 2005. Combination of high-fat diet-fed and low-dose streptozotocin-treated rat: a model for type 2 diabetes and pharmacological screening. Pharmacol Res 52(4): 313-320.

SZENDROEDI J, PHIELIX E & RODEN M. 2011. The role of mitochondria in insulin resistance and type 2 diabetes mellitus. Nat Rev Endocrinol 8(2): 92-103.

TORRES-JACOME J, GALLEGO M, RODRÍGUEZ-ROBLEDO JM, SANCHEZ-CHAPULA JA & CASIS O. 2013. Improvement of the metabolic status recovers cardiac potassium channel synthesis in experimental diabetes. Acta Physiol (Oxf) 207(3): 447-459.

VAAG A & LUND SS. 2007. Non-obese patients with type 2 diabetes and prediabetic subjects: distinct phenotypes requiring special diabetes treatment and (or) prevention? Appl Physiol Nutr Metab 32(5): 912-920.

WANG CH, WANG CC & WEI YH. 2010. Mitochondrial dysfunction in insulin insensitivity: implication of mitochondrial role in type 2 diabetes. Ann N Y Acad Sci 1201: 157-165.

WU J, ZHANG R, TORREGGIANI M, TING A, XIONG H, STRIKER GE, VLASSARA H & ZHENG F. 2010. Induction of Diabetes in Aged C57B6 Mice Results in Severe Nephropathy. Am J Pathol 176(5): 2163-2176.

ZHAO G, DHARMADHIKARI G, MAEDLER K & MEYER-HERMANN M. 2014. Possible role of interleukin-1β in type 2 diabetes onset and implications for anti-inflammatory therapy strategies. PLoS Comput Biol 10(8): e1003798.

ZHENG Y, LEY SH & HU FB. 2018. Global aetiology and epidemiology of type 2 diabetes mellitus and its complications. Nat Rev Endocrinol 14(2): 88-98.

ZIMMET P, ALBERTI KG & SHAW J. 2001. Global and societal implications of the diabetes epidemic. Nature 414(6865): 782-787.

SUPPLEMENTARY MATERIAL

Table SI. Primers sequences used in qRT-PCR to evaluate mRNAs expression.

AINHOA R. DE YURRE[1]
https://orcid.org/0000-0002-5920-7028

EDUARDA G.L. MARTINS[1,2]
https://orcid.org/0000-0003-0012-7514

MICAELA LOPEZ-ALARCON[1]
https://orcid.org/0000-0002-8700-9600

BRUNO CABRAL[1]
https://orcid.org/0000-0002-6783-1138

NARENDRA VERA[1]
https://orcid.org/0000-0001-7247-2697

JARLENE A. LOPES[1]
https://orcid.org/0000-0003-3194-2845

ANTONIO GALINA[2]
https://orcid.org/0000-0003-2862-8820

CHRISTINA M. TAKIYA[1]
https://orcid.org/0000-0002-8019-628X

RAFAEL S. LINDOSO[1]
https://orcid.org/0000-0002-7297-0781

ADALBERTO VIEYRA[1,3,4]
https://orcid.org/0000-0002-8009-7273

OSCAR C. SÁENZ[5]
https://orcid.org/0000-0002-6219-3317

EMILIANO MEDEI[1,4]
https://orcid.org/0000-0002-0044-1311

[1]Instituto de Biofísica Carlos Chagas Filho, Universidade Federal do Rio de Janeiro, Avenida Carlos Chagas Filho, 373, Ilha do Fundão, 21941-902 Rio de Janeiro, RJ, Brazil

[2]Instituto de Bioquímica Médica Leopoldo de Meis, Universidade Federal do Rio de Janeiro, Avenida Carlos Chagas Filho, 373, Ilha do Fundão, 21941-902 Rio de Janeiro, RJ, Brazil

[3]Programa de Pós-Graduação em Biomedicina Translacional, Universidade Grande Rio, Rua Professor José de Souza Herdy, 1160, 25071-202 Duque de Caxias, RJ, Brazil

[4]Centro Nacional de Biologia Estrutural e Bioimagem-CENABIO, Universidade Federal do Rio de Janeiro, Avenida Carlos Chagas Filho, 373, Ilha do Fundão, 21941-902 Rio de Janeiro, RJ, Brazil

[5]Departamento de Fisiologia, Faculdade de Farmacia, Universidade do País Vasco (UPV-EHU), Paseo de la Universidad 7, 01006, Vitoria-Gasteiz, Spain

Correspondence to: **Emiliano Medei**
E-mail: emedei70@biof.ufrj.br

Author contributions

EM and OCS conceived the project, designed the experiments and contribute to manuscript writing. ARY performed the experiments, analysed the data, prepared the figures and write the manuscript. EGLM performed mitochondria experiments and analysed the data obtained. MLA contributed to the renal data acquisition and analysis and performed cytokines measurements. BC performed WB experiments and analysed the data obtained. NV contribute to immunofluorescence data acquisition. AG and AV participated to study interpretation and revised the manuscript. CMT conducted immunofluorescence data acquisition and analysis and RSL and JAL performed renal biochemical experiments and analysed the data obtained. All authors read and approved the final manuscript.